

## Effect of asymmetric Schottky barrier on GaN-based metal-semiconductor-metal ultraviolet detector

Dabing Li, Xiaojuan Sun, Hang Song, Zhiming Li, Hong Jiang et al.

Citation: *Appl. Phys. Lett.* **99**, 261102 (2011); doi: 10.1063/1.3672030

View online: <http://dx.doi.org/10.1063/1.3672030>

View Table of Contents: <http://apl.aip.org/resource/1/APPLAB/v99/i26>

Published by the [American Institute of Physics](#).

---

### Related Articles

Photovoltaic infrared detection with p-type graded barrier heterostructures

*J. Appl. Phys.* **111**, 084505 (2012)

Unusual photoresponse of indium doped ZnO/organic thin film heterojunction

*Appl. Phys. Lett.* **100**, 162104 (2012)

Mid-wave infrared HgCdTe nBn photodetector

*Appl. Phys. Lett.* **100**, 161102 (2012)

Note: Characterization of CaF<sub>2</sub>/acetone bandpass photon detector with Kr filter gas

*Rev. Sci. Instrum.* **83**, 046107 (2012)

Note: Improved sensitivity of photoreflectance measurements with a combination of dual detection and electronic compensation

*Rev. Sci. Instrum.* **83**, 046105 (2012)

---

### Additional information on *Appl. Phys. Lett.*

Journal Homepage: <http://apl.aip.org/>

Journal Information: [http://apl.aip.org/about/about\\_the\\_journal](http://apl.aip.org/about/about_the_journal)

Top downloads: [http://apl.aip.org/features/most\\_downloaded](http://apl.aip.org/features/most_downloaded)

Information for Authors: <http://apl.aip.org/authors>

## ADVERTISEMENT

<p>INSTRUMENTS FOR ADVANCED SCIENCE</p> 			
<b>Gas Analysis</b> dynamic measurement of reaction gas streams catalysis and thermal analysis molecular beam studies dissolved species probes fermentation, environmental and ecological studies	<b>Surface Science</b> UHV TPD SIMS end point detection in ion beam etch elemental imaging - surface mapping	<b>Plasma Diagnostics</b> plasma source characterisation etch and deposition process reaction kinetic studies analysis of neutral and radical species	<b>Vacuum Analysis</b> partial pressure measurement and control of process gases reactive sputter process control vacuum diagnostics vacuum coating process monitoring
<p>contact Hiden Analytical for further details: <a href="mailto:info@hiden.co.uk">info@hiden.co.uk</a> <a href="http://www.HidenAnalytical.com">www.HidenAnalytical.com</a> CLICK TO VIEW OUR PRODUCT CATALOGUE</p>			
			

# Effect of asymmetric Schottky barrier on GaN-based metal-semiconductor-metal ultraviolet detector

Dabing Li,<sup>1,a)</sup> Xiaojuan Sun,<sup>1,2</sup> Hang Song,<sup>1</sup> Zhiming Li,<sup>1</sup> Hong Jiang,<sup>1</sup> Yiren Chen,<sup>1,2</sup> Guoqing Miao,<sup>1</sup> and Bo Shen<sup>3</sup>

<sup>1</sup>State Key Laboratory of Luminescence and Applications, Changchun Institute of Optics, Fine Mechanics and Physics, Chinese Academy of Sciences, 3888 Dongnanhu Road, Changchun 130033, People's Republic of China

<sup>2</sup>Graduate School of the Chinese Academy of Sciences, Beijing 100039, People's Republic of China

<sup>3</sup>State Key Laboratory of Artificial Microstructure and Mesoscopic Physics, School of Physics, Peking University, Beijing 100871, People's Republic of China

(Received 26 July 2011; accepted 2 December 2011; published online 27 December 2011; corrected 28 December 2011)

An asymmetric Schottky barrier metal-semiconductor-metal (MSM) ultraviolet (UV) detector with Ni/GaN/Au structure was designed and the effect of the asymmetric Schottky barrier on the detector response was investigated. This detector had response at 0 V bias and increased responsivity when a positive bias was applied to the Ni/GaN contact; however, the internal gain disappeared when a negative bias was applied to this point. This contrasts with a symmetric Ni/GaN/Ni Schottky barrier MSM UV detector which had no internal gain under positive/negative bias and almost no response at 0 V bias. The improved performance of the asymmetric Schottky barrier detector was because of the lower work function of Au causing reduction of Schottky barrier and hence enhancing a hole-accumulating and trapping process, which resulted in internal gain. © 2011 American Institute of Physics. [doi:10.1063/1.3672030]

Ultraviolet (UV) detectors have wide application fields such as solar UV monitoring, source calibration, flame sensors, and biological detection.<sup>1</sup> GaN and its alloys are very promising semiconductor materials for fabricating UV detectors by virtue of their direct wide bandgap, high saturation velocity, and excellent thermal and chemical stability. So far, various types of GaN-based detectors have been investigated, such as p-i-n detector,<sup>2</sup> Schottky barrier detector,<sup>3,4</sup> and metal-semiconductor-metal (MSM) detector.<sup>5–9</sup> Although the normal GaN MSM detector cannot operate at zero bias, it shows potential for high responsivity, low dark current, and low noise. In addition, GaN MSM detectors simplify the growth and fabrication processes since *n*- and *p*-type doped layers are not necessary. However, many factors, e.g., high-density defects and the Schottky barrier, affect the performance of the GaN-based UV detector. Detailed studies of the effect of high-density defects on the performance of GaN MSM UV detector have been reported.<sup>8,10</sup> The effect of the Schottky barrier on ZnO-based MSM UV detectors has also been reported.<sup>11</sup> However, the influence of the Schottky barrier on the GaN-based MSM detector has not been studied very well. In this paper, a GaN-based MSM UV detector with intentionally asymmetric Schottky barrier made by using different kinds of Schottky contact metal, Ni and Au, for each side, was designed and investigated in detail. For comparison, a device with a symmetric Schottky barrier using Ni contacts was also fabricated and studied. With the asymmetric Schottky barrier, operation of the GaN-based MSM detector under zero bias is realized and internal gain in the GaN MSM detector is also observed.

The epilayer structure of our devices consisted of 2  $\mu\text{m}$ -thick undoped GaN, which was deposited on c-plane

sapphire substrates at 1050 °C by using metalorganic chemical vapor deposition. Prior to growing the undoped GaN, a  $\sim 25$  nm thick GaN buffer layer was deposited at 550 °C. Trimethylgallium and ammonia were used as Ga and N sources, respectively. The room temperature carrier concentration for the active GaN layer was about  $3 \times 10^{16} \text{ cm}^{-3}$  and its dislocation density was about  $3 \times 10^9 \text{ cm}^{-2}$ . For the GaN-based MSM detector with different Schottky contact metals, shown schematically in the inset of Fig. 1, Ni (80 nm) was deposited first by electron-beam evaporation and then lift-off processes were used to make one side of the MSM structure. Then the other Schottky contact was fabricated by a similar process.

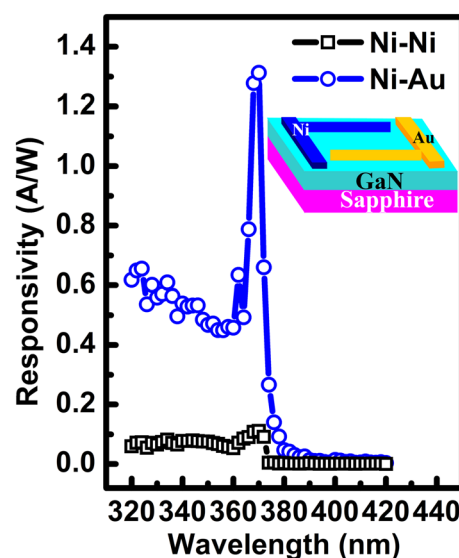


FIG. 1. (Color online) The room-temperature spectral responsivity of the GaN MSM detectors with Ni/GaN/Au and Ni/GaN/Ni structures at 5 V bias. The inset is the schematic device structure of the Ni/GaN/Au MSM detector.

<sup>a)</sup>Electronic mail: lidb@ciomp.ac.cn.

First, photolithographic alignment was carried out, then Au (80 nm) was deposited by thermal evaporation, and a second lift-off process was employed to complete the fabrication. The fingers were 5  $\mu\text{m}$  wide and 100  $\mu\text{m}$  long with 10  $\mu\text{m}$  wide spacing. Symmetric GaN MSM detectors with both Schottky contacts made of Ni (80 nm) were also prepared. Finally, all the samples were treated by rapid thermal annealing at 500  $^{\circ}\text{C}$  for 180 s. The voltage-dependent spectral responsivity and the current-voltage (I-V) characteristics were measured and the details of the measurements can be found in Ref. 8.

The responsivity as a function of wavelength for the Ni/GaN/Au (sample A) and Ni/GaN/Ni (sample B) UV detectors is shown in Fig. 1. The measurement was carried out at 5 V bias and the applied voltage referenced to the side of Ni Schottky contact for all measurements of sample A. Both detectors had sharp cut-offs at the band edge of GaN and showed a high responsivity. The peak responsivity values for the two detectors are 1.31 A/W and 0.11 A/W, respectively. As known, the theoretical limit of responsivity for an ideal GaN MSM structure is  $\sim 0.29$  A/W, thus the responsivity of sample A was much larger than the theoretical limit, which means that internal gain exists within this device. The product of the quantum efficiency and gain for the detectors could be calculated according to Eq. (1)<sup>12</sup>

$$R = \eta g \frac{q\lambda}{hc}, \quad (1)$$

where  $R$  is the responsivity;  $\eta$  is the quantum efficiency;  $g$  is the internal gain, and  $q$ ,  $\lambda$ ,  $h$ , and  $c$  are the electron charge, the incident light wavelength, Planck's constant, and the speed of light, respectively.  $\eta \times g$  was estimated to be about 4.52 and 0.38 at 5 V bias for samples A and B, respectively.

In order to explore the origin of such a high optical gain in sample A, the dark current-voltage (I-V) curves of the two detectors were measured, as shown in Fig. 2. The measurement began at  $-10$  V at the Ni/GaN Schottky contact for sample A. The I-V curves for both samples showed typical Schottky behavior, although the actual shapes of the curves, in particular their symmetry, were very different. The dark current was nearly symmetrical for sample B (Ni/GaN/Ni) and obviously asymmetric for sample A (Ni/GaN/Au). For

sample A, the dark current increased more than two orders of magnitude in the positive region compared to that in the negative region. As known, the MSM detector structure consists of two Schottky barriers, one in the forward direction and the other in the reverse direction. Under the assumption that almost all the potential drop was at the reverse junction, especially at higher bias, the dark current will be determined by the reverse junction, allowing an approximate calculation of the Schottky barrier height (SBH) at the reverse junction. Based on the thermal thermionic emission model,<sup>13</sup> the SBHs of the two samples under negative and positive biases were measured and calculated, which were about 0.81 and 0.71 eV, respectively, for Ni/GaN and Au/GaN of sample A and 0.82 and 0.82 eV for the two Ni/GaN contacts of sample B. The lower work function of Au compared to Ni metal might contribute to the lower SBH for Au/GaN compared to Ni/GaN. Thus, the asymmetric I-V behavior of sample A could be explained as follows: in the negative region, the Ni/GaN Schottky contact was under reverse junction and dominated the dark current and the SBH, resulting in dark current in this region being similar to that for sample B. In contrast, in the positive region, the Au/GaN contact determined the SBH and the dark current; the lower SBH and much larger dark current occurred because of the lower work function of Au and hole trapping process. In brief, the asymmetric Schottky barrier detector was caused by the lower work function of Au compared to Ni, which made holes drifted and accumulated under applied voltage. And then holes became trapped at the Au/GaN interface further causing lower SBH and, thus, larger dark current occurred.

To confirm this speculation, the voltage-dependent responsivity of sample A (Ni/GaN/Au interdigitated Schottky contact) was measured (Fig. 3(a)). The inset is the responsivity of sample A under zero bias; an obvious response (0.005 A/W) was observed under zero bias, arising from band bending caused by the different Schottky barrier heights of the Ni/GaN and Au/GaN interfaces. Meanwhile, the peak responsivity of the two samples is shown in Fig. 3(b). For sample A, when a positive voltage was applied at the Ni/GaN contact, the responsivity of this detector increased sharply, indicating that the internal gain played an important role. In contrast, when a negative voltage was applied to the Ni/GaN contact, the responsivity was almost

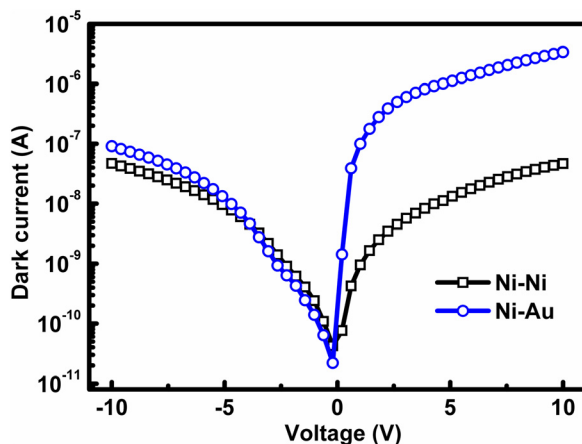


FIG. 2. (Color online) Dark I-V curves of the two GaN MSM detectors.

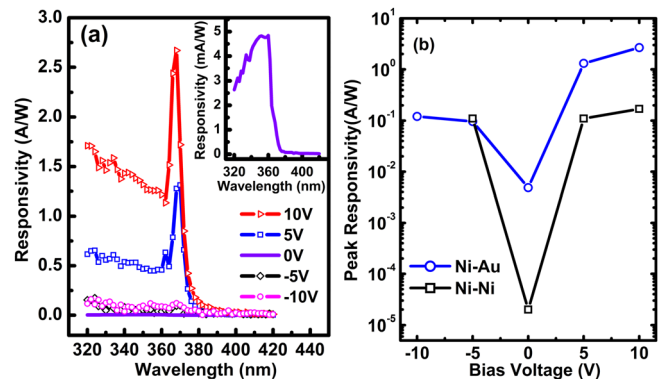


FIG. 3. (Color online) (a) The room-temperature spectral responsivity of the Ni/GaN/Au detector under different bias voltages. The inset is the spectral responsivity under 0 V bias. (b) The peak responsivity of the two types of detectors under different biases.



independent of the bias, implying that the gain was much smaller. However, for sample B, no obvious change was observed when changing the applied voltage, and almost no response was detected under zero bias. These results further demonstrated that the asymmetric Schottky barrier causes the high responsivity of sample A.

To explain this voltage-dependent responsivity, a schematic illustration of the bandgap alignment in this detector is shown in Fig. 4. Since the current under illumination can be expressed by Eq. (2),

$$I_{\text{illumination}} = AA^*T^2 \exp\left(-\frac{\phi_b - \Delta\phi_b}{KT}\right) \left(\exp \frac{qV}{nKT} - 1\right) - I_\lambda, \quad (2)$$

where  $A$  is the area of the photodetector,  $A^*$  is the effective Richardson constant,  $\phi_b$  is the Schottky barrier height, and  $\Delta\phi_b$  is the reduction of  $\phi_b$  under a certain condition,  $q$  is the electron charge,  $V$  is the applied voltage,  $n$  is the ideality factor, and  $I_\lambda$  is the primary current. Considering the dark current,

$$I_{\text{dark}} = AA^*T^2 \exp\left(-\frac{\phi_b}{KT}\right) \left(\exp \frac{qV}{nKT} - 1\right). \quad (3)$$

Then the responsivity could be deduced from Eqs. (2) and (3),

$$R = \frac{\exp\left(\frac{\Delta\phi_b}{KT}\right) I_{\text{dark}} - I_\lambda}{W}, \quad (4)$$

where  $W$  is the light intensity. Equation (4) shows that lowering the Schottky barrier would enhance the photoresponse.

As illustrated in Fig. 4(a), when a positive voltage was applied to the Ni, the photogenerated holes drifted to the Au/GaN interface and then the holes accumulated at surface/interface traps and produced net positive charge  $Q_s$ . Since the sum of the positive depletion charge due to uncompensated donors and the trapped holes creating charge must be equal to the metal negative charge, the depletion charge must have decreased if charged surface states occurred. This indicated that the built-in voltage would be reduced corre-

spondingly, leading to a decrease in the Schottky barrier height,  $\Delta\phi_{b1}$ ,

$$\Delta\phi_{b1} = \frac{Q_s d}{2\epsilon\epsilon_0}, \quad (5)$$

where  $d$  is the depletion width at the Au/GaN interface,  $\epsilon_0$  is the permittivity of free space, and  $\epsilon_s$  is the relative dielectric permittivity. Furthermore, the lower work function of Au compared to Ni further reduced the Schottky barrier height  $\Delta\phi_{b2}$  at the Au/GaN interface; both these factors explain the high responsivity observed when positive voltage was applied to Ni. However, when a negative voltage was applied to Ni, illustrated in Fig. 4(b), the Ni/GaN reverse junction dominated the behavior of the GaN MSM detector. Since Ni has a high work function, there will be no obvious net charge associated with trapped holes, and hence no reduction in the Schottky barrier height at the Ni/GaN interface, leading to the lower dark current as shown in Fig. 2 and absence of internal gain (Fig. 3(b)).

In conclusion, a high responsivity of 1.31 A/W at 5 V bias, zero-bias operation, and bias direction-dependent detection was realized by using an asymmetric Schottky barrier Ni/GaN/Au MSM UV detector. The responsivity varied with the polarity of the applied voltage; high responsivity with internal gain was obtained when a positive voltage was applied at the Ni/GaN contact, but this gain was absent when a negative voltage was applied. Both the metal work function and the hole trapping process contributed to the increase in responsivity. Therefore, this study provides a route for design of a high responsivity MSM UV detector and may broaden its application fields due to its zero-bias operation and bias direction-dependent responsivity.

This work was partly supported by the National Key Basic Research Program of China (Grant Nos. 2011CB301901, 2012CB619303, and 2012CB619306), the National Natural Science Foundation of China (Grant Nos. 51072195 and 51072196), and the National High-tech R&D Program of China (863 Program, Grants No. 2011AA03A111).

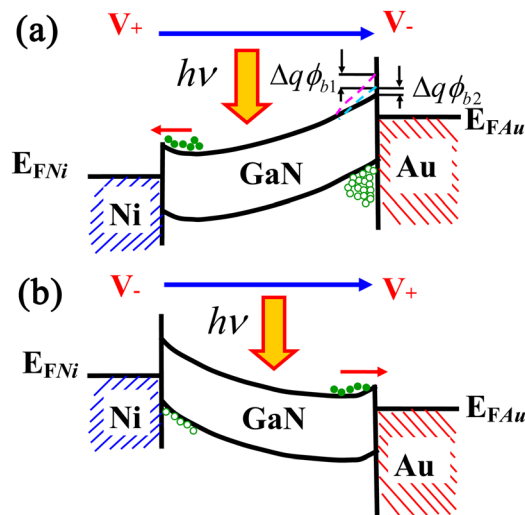


FIG. 4. (Color online) Schematic illustration of the bandgap alignment of the Ni/GaN/Au detector under different direct biases.

<sup>1</sup>M. Razeghi and A. Rogalski, *J. Appl. Phys.* **79**, 7433 (1996).

<sup>2</sup>B. Butun, T. Tut, E. Ulker, T. Yelboga, and E. Ozbay, *Appl. Phys. Lett.* **92**, 033507 (2008).

<sup>3</sup>Q. Chen, J. W. Yang, A. Osinsky, S. Gangopadhyay, B. Lim, M. Z. Anwar, M. Asif Khan, D. Kuksenkov, and H. Temkin, *Appl. Phys. Lett.* **70**, 2277 (1997).

<sup>4</sup>O. Katz, V. Garber, B. Meyler, G. Bahir, and J. Salzman, *Appl. Phys. Lett.* **80**, 347 (2002).

<sup>5</sup>J. Lia, Y. Xu, T. Y. Hsiang, and W. R. Donaldson, *Appl. Phys. Lett.* **84**, 2091 (2004).

<sup>6</sup>M. Mosca, J. L. Reverchon, F. Omnes, and J. Y. Duboz, *J. Appl. Phys.* **95**, 4367 (2004).

<sup>7</sup>J. L. Pau, C. Rivera, E. Muñoz, E. Calleja, U. Schuhle, E. Frayssinet, B. Beaumont, J. P. Faurie, and P. Gibart, *J. Appl. Phys.* **95**, 8275 (2004).

<sup>8</sup>D. B. Li, X. J. Sun, H. Song, Z. M. Li, Y. R. Chen, G. Q. Miao, and H. Jiang, *Appl. Phys. Lett.* **98**, 011108 (2011).

<sup>9</sup>X. J. Sun, D. B. Li, H. Jiang, Z. M. Li, H. Song, Y. R. Chen, and G. Q. Miao, *Appl. Phys. Lett.* **98**, 121117 (2011).

<sup>10</sup>G. Koley and M. G. Spencer, *Appl. Phys. Lett.* **78**, 2873 (2001).

<sup>11</sup>J. S. Liu, C. X. Shan, B. H. Li, Z. Z. Zhang, C. L. Yang, D. Z. Shen, and X. W. Fan, *Appl. Phys. Lett.* **97**, 251102 (2010).

<sup>12</sup>S. M. Sze and K. K. Ng, *Physics of Semiconductor Devices*, 3rd ed. (Wiley, Hoboken, 2007).

<sup>13</sup>M. Razeghi and A. Rogalski, *J. Appl. Phys.* **79**, 7433 (1996).